

---

# MUJO: MULTIMODAL JOINT FEATURE SPACE LEARNING FOR HUMAN ACTIVITY RECOGNITION

---

Stefan Gerd Fritsch<sup>†\*1</sup>, Cennet Oguz<sup>‡\*2</sup>, Vitor Fortes Rey<sup>1,3</sup>, Lala Ray<sup>1</sup>, Maximilian Kiefer-Emmanouilidis<sup>1,3,4</sup>,  
and Paul Lukowicz<sup>1,3</sup>

<sup>1</sup>Embedded Intelligence, DFKI, 67663 Kaiserslautern, Germany

<sup>2</sup>Multilinguality and Language Technology, DFKI, 66123 Saarbrücken, Germany

<sup>3</sup>Department of Computer Science, RPTU Kaiserslautern-Landau, 67663 Kaiserslautern, Germany

<sup>4</sup>Department of Physics, RPTU Kaiserslautern-Landau, 67663 Kaiserslautern, Germany

## ABSTRACT

Human Activity Recognition is a longstanding problem in AI with applications in a broad range of areas: from healthcare, sports and fitness, security, and human computer interaction to robotics. The performance of HAR in real-world settings is strongly dependent on the type and quality of the input signal that can be acquired. Given an unobstructed, high-quality camera view of a scene, computer vision systems, in particular in conjunction with foundational models (e.g., CLIP), can today fairly reliably distinguish complex activities. On the other hand, recognition using modalities such as wearable sensors (which are often more broadly available, e.g. in mobile phones and smartwatches) is a more difficult problem, as the signals often contain less information and labeled training data is more difficult to acquire. In this work, we show how we can improve HAR performance across different modalities using multimodal contrastive pretraining. Our approach MuJo (Multimodal Joint Feature Space Learning), learns a multimodal joint feature space with video, language, pose, and IMU sensor data. The proposed approach combines contrastive and multitask learning methods and analyzes different multitasking strategies for learning a compact shared representation. A large dataset with parallel video, language, pose, and sensor data points is also introduced to support the research, along with an analysis of the robustness of the multimodal joint space for modal-incomplete and low-resource data. On the MM-Fit dataset, our model achieves an impressive Macro  $F_1$ -Score of up to 0.992 with only 2% of the train data and 0.999 when using all available training data for classification tasks. Moreover, in the scenario where the MM-Fit dataset is unseen, we demonstrate a generalization performance of up to 0.638.

## 1 Introduction

Perceiving and interpreting human activity is a core functionality of intelligent systems with applications in a broad range of areas: from healthcare Tan et al. [2021] through sports and fitness Host and Ivašić-Kos [2022], Nadeem et al. [2020], security Sunil et al. [2021] to robotics Piyathilaka and Kodagoda [2015]. A basic capability needed to facilitate such functionality is the identification of concrete human actions from the system’s sensory input, referred to as Human Activity Recognition (HAR) Hamad et al. [2023]. In general, HAR is a difficult problem, especially when applied to uncontrolled real-life environments, where it must contend with the variability of human actions and the open-ended variations in environmental conditions. In such settings, the performance of HAR systems is strongly dependent on the available input modalities. Recent advances in Computer Vision, particularly with Large Vision Language Models (VLMs) Radford et al. [2021], Achiam et al. [2023], have enabled impressive performance when given sufficiently high-quality images. In many cases, merely feeding images to publicly available tools such as GPT-4 can result in

<sup>†</sup>Corresponding Author. Email: stefan\_gerd.fritsch@dfki.de.

<sup>‡</sup>Corresponding Author. Email: cennet.oguz@dfki.de.

\*Equal contribution.

*This work was submitted to a conference on April 25, 2024.*

accurate description of scenes involving complex and subtle activities. However, in real-life settings, such images are not always available; either due to a lack of cameras or because of privacy concerns. Much more broadly available input modalities are wearable sensors, in particular, Inertial Measurement Units (IMUs), which are ubiquitous in smartphones, smartwatches or even earbuds, all of which people carry with them on a daily basis. Unfortunately, achieving acceptable recognition performance with such sensors is a much more difficult problem due to two factors:

1. **Information ambiguity:** An IMU (which is essentially a motion sensor) in a smartwatch on the wrist or in a smartphone in a pocket contains much less detailed information about the user’s activity than a high-quality picture.
2. **Lack of training data:** The success of VLMs is built on the online availability of massive amounts of text/image data pairs, which can be used for training aligned representations. Although large amounts of unlabeled IMU data are increasingly becoming available Chan et al. [2024], labeled training data remains scarce.

The work presented in this paper, which aims to address the issues outlined previously, is founded on three key observations:

1. While the input modalities available during inference—the time when the system is utilized in the real world—may be constrained, the input modalities during training can be selected with much greater flexibility.
2. Representation learning facilitates knowledge transfer between modalities by aligning embedding spaces, in particular when synchronized training data is available.
3. Significant progress has recently been made in generating synthetic data for a variety of sensors from videos. For example, IMUTube Kwon et al. [2021] generates virtual gyroscope and accelerometer data from videos, while pose extraction methods like OpenPose Cao et al. [2017] and VideoPose3D Pavllo et al. [2019] are used to generate skeletal data of human activities. This enables the creation of synchronised video/sensor training data and through the alignment of video with text, it facilitates the synchronization of sensor data with textual descriptions.

Based on the above considerations, we propose a multimodal contrastive pretraining method that creates a joint representation between videos, video-derived poses, synthetic IMU data created from videos using IMUTube Kwon et al. [2021], and textual descriptions. Our approach, which we refer to as MuJo, aims to utilize the complementary information of each modality to improve the performance for both unimodal and multimodal inference. In particular, we show that our method dramatically reduces the need for labeled training data for downstream tasks. Thus, on the well-known MM-Fit dataset Strömbäck et al. [2020], when using all available training data, our method improves the recognition rate (Macro  $F_1$ -Score) from 0.973 to 0.999 in the multimodal case (encompassing all of the above modalities), from 0.957 to 0.988 for poses, and from 0.727 to 0.863 for video alone. For sensor data, the performance of our method is slightly worse (0.798 as opposed to 0.822), which is due to the fact that MM-Fit uses real, rather than simulated sensor data. However, when using just 2% of the available data for training, the baseline with sensors has an  $F_1$ -Score of just 0.378 whereas our systems achieves a reasonable 0.627 (see section 6.2 for details). The multimodal  $F_1$ -Score is 0.819 in the baseline, while our method raises it to 0.992.

Overall, the key contributions of this work can be summarized as follows:

- Development of a large fitness dataset<sup>1</sup> with parallel video, language (i.e., labels of video clips, captions uttered by the instructor in the video clip, and precise descriptions of the exercises generated by GPT-3.5), pose, and simulated IMU data points.
- Learning of an effective joint space for the modalities of text, video, pose, and sensor by leveraging the contrastive loss.
- Analysis of usefulness and generalizability of multimodal joint space for each modality and their combination, as well as the benefits of pretraining when a low amount of data is available for the target task.

## 2 Related Work

### 2.1 Human Activity Recognition

**Unimodal activity recognition.** Unimodal activity recognition has been extensively studied in HAR. Various approaches have been proposed to address this task, and they can be broadly categorized into two groups: hand-crafted

<sup>1</sup>Available after publication at link.

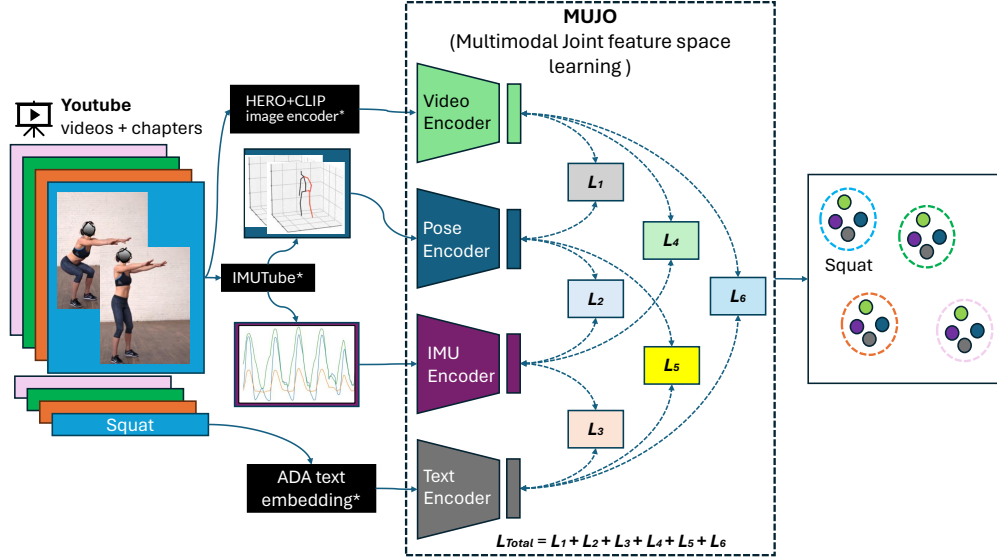


Figure 1: The pipeline depicting our data construction process and training of MuJo for multimodal joint feature space learning. The asterisk \* indicates that the input is being pre-calculated (frozen) and is not optimization during the training process.

feature-based and deep learning-based methods. Hand-crafted feature-based methods rely on extracting low-level features from the input data and designing a classifier to recognize activities. For instance, in accelerometer-based activity recognition Kwapisz et al. [2011], features such as mean, standard deviation, and energy of the acceleration signal are often used to capture the characteristics of different activities. Popular classifiers used in this approach include decision trees, support vector machines, and k-nearest neighbors. Deep learning-based methods, on the other hand, use neural networks to learn features and recognize activities from raw input data. Convolutional neural networks (CNNs) and recurrent neural networks (RNNs) are two popular types of neural networks used in this approach. CNNs are commonly used for image-based activity recognition Strömbäck et al. [2020], Ordóñez and Roggen [2016], being combined with RNNs in some cases Ordóñez and Roggen [2016]. Despite the success of unimodal activity recognition, it is often limited by the fact that a single modality of input data may only capture some of the necessary information about the activity, leading to lower recognition accuracy. Therefore, multimodal activity recognition, which combines information from multiple sources, has gained increasing attention in recent years.

**Multimodal activity recognition.** Multimodal activity recognition recognizes human activities using information from multiple modalities, such as IMU data, audio, and video Mekruksavanich and Jitpattanakul [2022], Ijaz et al. [2022]. These features can then be combined using fusion methods such as early fusion or late fusion Duhme et al. [2022]. Some studies have also focused on domain adaptation, where the goal is to recognize activities in a new environment using data from a different environment Plananamente et al. [2022]. In such cases, transfer learning techniques can adapt the model to the new environment using a small amount of labeled data. Overall, multimodal activity recognition has shown promising results, with improved accuracy compared to unimodal approaches. However, challenges in data fusion, feature extraction, and model selection still need to be addressed to improve the performance of multimodal activity recognition systems Islam et al. [2022].

## 2.2 Representation Learning for Human Activities

**Representation learning with proxy tasks.** Different modalities, e.g., natural language, visual inputs, or sensor signals, often complement a common concept. A key challenge of multimodal feature representation is exploring efficient methods for multimodal fusion with the given modalities to avoid missing modal features. We can differentiate the representation learning methods in two aspects: learning objectives and fusing the learned features in a joint space. In learning objectives, various approaches have been proposed to learn multimodal representations by formulating proxy tasks such as reconstruction, completion Seo et al. [2021], Sun et al. [2019], matching/alignment Li et al. [2020], Miech et al. [2020], and ordering tasks Li et al. [2020]. Generating one feature vector with multimodal inputs for a common concept is a crucial problem of multimodal representation learning. Simple methods like concatenating Hu et al. [2018], Strömbäck et al. [2020] learned uni-modal feature vectors have been extensively explored to enhance the

performance of downstream tasks. These methods involve combining feature vectors from a single modality, such as text or image, to create more informative representations that can be used for various tasks. Thereafter, Zadeh et al. proposed a tensor fusion network in Zadeh et al. [2017]. Lu et al. proposed a co-attention mechanism based on the transformer architecture in Lu et al. [2019] for efficient cross-modality learning.

**Representation via contrastive learning.** Contrastive Learning is as an efficient self-supervised framework applied across multiple domains, which learns similar/dissimilar representations from data that are organized into similar/dissimilar pairs. Recently, Radford et al. presented a novel approach, known as CLIP Radford et al. [2021], to jointly represent images and text descriptions by leveraging contrastive loss with the similarity of image-text pairs. CLIP learns two feature spaces with two encoders, i.e., image and text encoders, then projects the learned features into a shared latent space with contrastive loss. Contrastive learning, a joint feature space of text-image pairs, has been extended to other modalities. For example, video-text data has attracted studies on shared space of video-text features Xu et al. [2021], Xue et al. [2022], text-to-video generation Singer et al. [2022]. Thereafter, MotionCLIP Tevet et al. [2022] trained an encoder to find the proper embedding of an input sequence in CLIP space, and a decoder that generates the most fitting motion to a given CLIP space. Following that, IMU2CLIP Moon et al. [2022] has been proposed to learn a joint space to align Inertial Measurement Unit (IMU) motion sensor recordings with video and text, by projecting them into the joint representation space.

Studies in action recognition Aggarwal and Ryoo [2011], Li et al. [2020], Wang et al. [2021], Sun et al. [2022], Morshed et al. [2023] can also significantly enhance the field of recognition in fitness activities, despite action recognition emphasis on a broad spectrum of actions such as “cutting the potato” and “cleaning the drawer”, among others. Certain investigations in action recognition also endeavor to acquire knowledge of the feature space through contrastive learning methodologies, exemplified by initiatives such as HERO Li et al. [2020] and ActionCLIP Wang et al. [2021].

The achievements discussed in the aforementioned studies have shown contrastive learning has a high impact on extracting a joint space with similar and dissimilar pairs. Hence, the contrastive learning methodology employed in this study is utilized to acquire knowledge of the feature space pertaining to fitness activities. Contrary to previous work, we extend this line of work on contrastive learning to a unique multimodal setting that utilizes more than two modalities, such as video, IMU sensors, poses, and text, within a multitask training manner in an end-to-end training paradigm similar to ImageBind Girdhar et al. [2023]. Thus, our model and data provide a cross-modal classification opportunity.

### 3 Dataset

#### 3.1 Video Collection

YouTube provides chapters within a video, each with its preview, providing information and context for different parts of the video. Video owner can manually add chapters to their uploaded videos or rely on automatic chapter generation. We manually collect 1212 fitness videos with pre-annotated video chapters. Additionally, we retrieve the captions automatically generated by YouTube. Our videos include only one tutor who teaches how to do fitness exercises (e.g., “squat with dumbbells”, “sit-ups”, “side deep squats”, etc.). Thus, the exercise videos provide instructions for the activities while showing the activities clearly. The annotation does not include predefined categories or labels. Each video owner annotates the activity segment of the videos with their personal preferences, such as “deep squats with dumbbells”, “high jump squats”, etc., instead of only “squats”. Given the temporal boundaries of the activity within each video, we split the videos in shorter activity clips along with their corresponding chapters and caption segments.

Since workout exercises are typically short, activity videos that are too long often contain multiple exercises and, thus, incorrect chapter labels. Hence, we only keep exercises shorter than 2 minutes and discard more extended exercises. After that, the dataset consists of 10,695 (video, chapter, caption) samples.

#### 3.2 Dataset Construction

We convert all videos to 720p resolution and 50 frames per second via FFmpeg’s adaptive overlapped block motion compensation with bidirectional motion estimation. Then, we extract simulated sensor data, poses, as well as a variety of video and text features. Video features are extracted with HERO Li et al. [2020] utilizing CLIP Radford et al. [2021] and S3D Xie et al. [2018] embeddings. On the textual side, we apply several normalization strategies to the raw chapters such as replacing abbreviations within the text (e.g., changing “l” to “left” and “r” to “right”) as well as removing stop words, numbers, and a few special symbols from a predefined list. Further, we use GPT 3.5 to generate detailed descriptions of the exercises. We then extract multiple text features with different models, including OpenAI’s text-embedding-ada-002 embedding model (ADA), CLIP, BERT Devlin et al. [2018], as well as language features and motion tokens extracted with Text2Motion Transformer Guo et al. [2022]. We apply IMUTube Kwon et al.



Figure 2: Word cloud highlighting the most frequent chapter labels in our dataset.

[2021] to generate virtual gyroscope and accelerometer data for sensors placed on all 16 joint nodes. We also use the implementation of IMUTube to extract 3D poses from the videos, which utilizes OpenPose followed by VideoPose3D for 3d pose lifting.

Since IMUTube fails to extract sensor data for 884 videos, we exclude these sequences. We use the remaining 9811 exercises as our dataset and split it into train (8,518 videos), validation (946 videos) and test (347 videos) sets. Since workout session videos typically start with an introductory sequence and conclude with a farewell, we discard the initial and final 15%<sup>2</sup> of each video. Despite these filtering steps, we receive a large dataset totaling around 78 hours in length. Instances are generated using sliding windows  $x_i$  of 100 frames in length (i.e., 2 seconds) with 50 frames overlap from the videos. We found this size suitable for fitness exercises as a 2 second window generally captures enough meaningful information regarding the subject’s movements.

In summary, our dataset comprises a large collection of short fitness activity clips containing video features, poses, synthetic IMU data, chapter labels, captions, and GPT-generated descriptions as well as several types of features extracted from these text modalities.

## 4 Method

Our method leverages multimodal information for HAR pretraining. The fundamental idea is that the extracted information for a short video interval should be similar, as it represents the same activity from various perspectives. For each window, we extract features for each modality, which means our data consists of  $\mathcal{X}^m = \{x_m^1, \dots, x_m^N\}$  where  $x_m^i$  is the feature for modality  $m$  at time interval  $i$ . We use as modalities

- $\mathcal{X}^{pose}$ : The sequence of 3D poses for the subject extracted using VideoPose3D.
- $\mathcal{X}^{video}$ : Video features extracted with HERO Li et al. [2020] utilizing CLIP Radford et al. [2021] embeddings.
- $\mathcal{X}^{acc}$ : Simulated accelerometer data of both wrists generated by ImuTube Kwon et al. [2021].
- $\mathcal{X}^{text}$ : Embeddings extracted using OpenAI’s ADA model from YouTube’s chapter information with a lightweight normalization process removing a few special symbols and replacing abbreviations within the text.

Each modality  $m$  has its own encoder network  $e_m$  and projection layers  $p_m$ . Thus,  $rep_m(x_m) = p_m(e_m(v_m))$  serves as our representation for a vector  $v_m$  of modality  $m$  in our shared representation space. We learn this shared space

<sup>2</sup>This value has proven to be effective in experimental investigations.

between modality representations using pair-wise contrastive learning, as depicted in Figure 1. First, for all possible  $(m_a, m_b)$  modality pairs, we compute similarities using

$$\text{sim}(v_a, v_b) = \frac{\text{rep}_{m_a}(v_a) \times \text{rep}_{m_b}(v_b)^\top}{\|\text{rep}_{m_a}(v_a)\| \cdot \|\text{rep}_{m_b}(v_b)\|} \quad (1)$$

Then, those similarities are softmax-normalized within the batch to calculate the loss between the two modalities

$$\mathcal{L}_c(x_a, x_b) = - \sum_i \log \frac{\exp(\text{sim}(x_a^i, x_b^i)/\tau)}{\sum_j \exp(\text{sim}(x_a^i, x_b^j)/\tau)}. \quad (2)$$

where  $x_a$  and  $x_b$  correspond to aligned batch data for modalities  $a$  and  $b$ , respectively, and  $\tau$  is the temperature hyper-parameter. Since we calculate losses between all modalities, our total loss amounts to

$$\mathcal{L}_{total} = \frac{1}{\binom{M}{2}} \sum_{m_a, m_b} (\mathcal{L}_c(x_{m_a}, x_{m_b}) + \mathcal{L}_c(x_{m_b}, x_{m_a})), \quad (3)$$

where  $M$  is the total number of modalities (in our case 4). An example can be seen in Figure 1.

Regarding the structure of our encoders, we utilize a model with a single fully connected layer for  $e_{text}$  and two fully connected layers for  $e_{video}$ . For  $e_{pose}$  and  $e_{sensor}$ , we employ the CNN encoder architecture as described in Strömbäck et al. [2020]. The projection  $p_m$  is a two-layer fully connected model for all modalities  $m$ , mapping them to feature vectors of length 1280.

We apply a random search approach for hyperparameter selection. Our hyperparameters include learning rate, number and size of projection layers, dropout rates, and activation functions. We also experimented with various configurations of the loss function, specifically comparing using the text modality as an anchor and, hence, considering sensor-text, pose-text, and video-text loss pairs only versus incorporating all possible modality combinations into the loss. Encompassing all modality pairs together yielded superior results. We explored weighting the text modality higher than the others in the loss, but it did not have any observable effect on performance.

We also explored the use of S3D-based video embeddings, the gyroscope as sensor input, and the other text modalities and features described in Section 3.2 as inputs. However, since those configurations did not yield the best performance during the hyper-parameter search, we have omitted those results for the sake of brevity.

Dataset Type	Input Modality	Mean Macro $F_1$ -Score					
		Train Data: 2%			Train Data: 100%		
		Baseline	Ours (Frozen)	Ours	Baseline	Ours (Frozen)	Ours
Real-World	Sensor	.042 ± .013	<b>.206</b> ± .010	.190 ± .014	.154 ± .024	.259 ± .004	<b>.274</b> ± .010
	Pose	.094 ± .029	<b>.300</b> ± .011	.294 ± .021	.271 ± .024	<b>.388</b> ± .005	.366 ± .011
	Video	.026 ± .007	.076 ± .009	<b>.079</b> ± .008	.097 ± .009	.098 ± .005	<b>.126</b> ± .005
	Multimodal	.090 ± .014	.305 ± .014	<b>.309</b> ± .017	.186 ± .015	.381 ± .006	<b>.394</b> ± .009
Rendered	Sensor	.053 ± .011	<b>.180</b> ± .010	.165 ± .012	.181 ± .016	.246 ± .005	<b>.253</b> ± .011
	Pose	.086 ± .022	.277 ± .015	<b>.287</b> ± .017	.304 ± .016	.370 ± .005	<b>.404</b> ± .010
	Video	.048 ± .015	.071 ± .007	<b>.090</b> ± .015	.125 ± .033	.154 ± .005	<b>.177</b> ± .004
	Multimodal	.119 ± .018	.282 ± .017	<b>.288</b> ± .017	.272 ± .022	.386 ± .008	<b>.402</b> ± .014

Table 1: Comparison of classification results across all modalities evaluated on the FLAG3D test dataset. The table illustrates the mean Macro  $F_1$ -Scores and standard deviations when utilizing 2% and 100% of the training data. Results are presented for the baseline classifier versus our model, which is initialized with pretrained encoder and projection weights. The comparison includes scenarios with and without frozen encoders and projections during training of the classifier. Results demonstrating superior performance are highlighted in bold.

## 5 Experiments

We evaluate the performance of our methodology on the FLAG3D and MM-Fit datasets. On FLAG3D, we show performance in classification task whereas on MM-Fit, besides classification, we additionally evaluate the generalization performance of our representation in the scenario where the dataset is unseen and also compare unimodal versus multimodal training.

### 5.1 Classification

For classification, we utilize a classifier architecture  $C$  comprising one or multiple pretrained encoder(s)  $e$ , projection(s)  $p$ , and a classification head  $cl$  consisting of 2 layers. We contrast three scenarios: In the baseline setting, all weights are

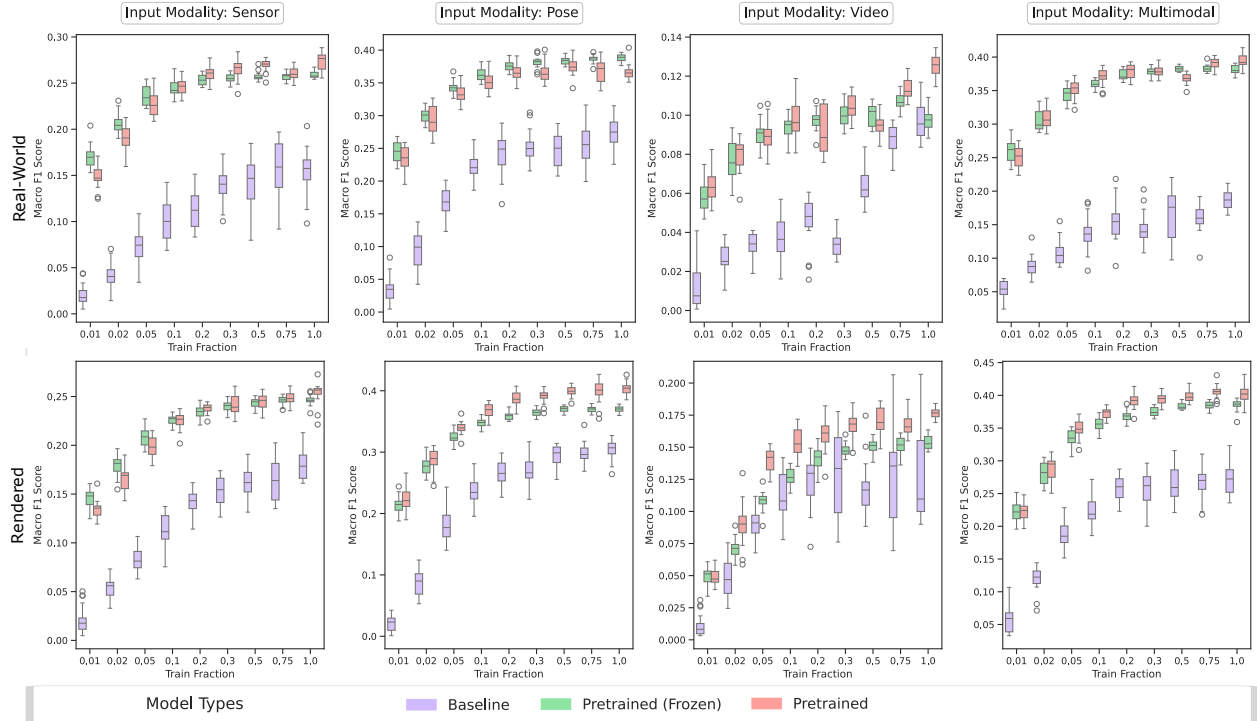


Figure 3: Boxplots visualizing the classification performance (Macro  $F_1$ -Score) across various training data fractions of the baseline model versus models with a pretrained encoder and projection, both frozen and unfrozen, on FLAG3D real-world (top) and rendered (bottom) datasets.

initialized randomly, meaning the model lacks any pretrained knowledge. In the subsequent scenarios, the encoder and projection head is initialized with weights from our pretrained model. In one case, the weights of the encoder and projection head are fixed (frozen), whereas in the other case, we fine-tune them during the classifier’s training process. We train the model with all possible input modalities, namely accelerometer, poses, and videos, separately. Furthermore, we experiment with multimodal input by providing all three modalities to the model and concatenating the outputs from the respective projections before feeding them into  $cl$ . In addition, we train with different proportions of the training data, ranging from one to 100 percent, with the training data being sampled per class to ensure balanced representation. To guarantee comparability of all results, we train each classifier  $C$  with the same settings: We utilize a learning rate of 0.0001 and training is conducted for a maximum of 200 epochs, incorporating early stopping after 25 epochs without improvement. We employ a weighted cross-entropy classification loss to address class imbalance, given by:

$$\mathcal{L}_{CL} = - \sum_{i=1}^n w_{y_i} y_i \log(C(x_i)), \quad (4)$$

where  $n$  is the number of classes,  $y_i$  is a one-hot encoded ground truth activity label and  $C(x_i)$  is the predicted label vector of  $C$  for input  $x_i$ , that is, the application of our  $cl$  classification layers to obtain  $cl(p(e(x_i)))$ . The weight  $w_{y_i} = \frac{\max(M)}{m_{y_i}}$  for class  $y_i$  is calculated by dividing the number of data samples of the largest class by the number of instances in class  $y_i$  itself. To ensure validity of the results, we train 20 models independently for each configuration, with the training data being randomly selected anew for each run (for proportions less than 100%) and the non-pretrained weights being reinitialized randomly.

### 5.1.1 FLAG3D

The FLAG3D Tang et al. [2023] dataset is a large-scale 3D fitness activity collection with language instruction of 60 categories. The dataset comprises (a) 7,200 3D activity sequences performed by 10 individuals acquired from an advanced MoCap system, (b) 172,800 2D RGB videos rendered from the 3D MoCap data including different scenes, avatars, and camera positions, and (c) 7,200 authentic videos of ten persons captured by cost-effective smartphones in both indoor and outdoor natural settings. Additionally, FLAG3D offers comprehensive and meticulously crafted sentence-level language instructions for each fitness activity.

	Input Modality	Calibration	Mean Macro $F_1$ -Score					
			Train Data: 2%			Train Data: 100%		
			Baseline	Ours (Frozen)	Ours	Baseline	Ours (Frozen)	Ours
Without "No Activity"	Sensor	No	.421 ± .040	.524 ± .029	<b>.529</b> ± .024	.554 ± .021	.557 ± .007	<b>.567</b> ± .008
		Unsupervised	.213 ± .038	<b>.385</b> ± .029	.383 ± .037	.462 ± .025	<b>.489</b> ± .007	.416 ± .039
		Supervised	.378 ± .099	.593 ± .028	<b>.627</b> ± .025	<b>.822</b> ± .035	.769 ± .008	.798 ± .015
	Pose	No	<b>.772</b> ± .068	—	—	<b>.901</b> ± .028	—	—
		Unsupervised	.731 ± .059	.836 ± .020	<b>.884</b> ± .023	.910 ± .030	.905 ± .013	<b>.933</b> ± .016
	Supervised	Supervised	.796 ± .089	.969 ± .008	<b>.977</b> ± .008	.957 ± .026	.983 ± .002	<b>.988</b> ± .007
		Video	No	.643 ± .051	.803 ± .016	<b>.830</b> ± .016	.727 ± .035	.860 ± .004
	Multimodal	No	<b>.798</b> ± .042	—	—	<b>.906</b> ± .030	—	—
Unsupervised		.719 ± .042	.908 ± .013	<b>.923</b> ± .018	.809 ± .039	.927 ± .005	<b>.961</b> ± .008	
Supervised		.819 ± .048	.992 ± .004	<b>.992</b> ± .004	.973 ± .012	.997 ± .002	<b>.999</b> ± .001	
With "No Activity"	Sensor	No	.230 ± .022	.289 ± .014	<b>.316</b> ± .019	.328 ± .016	.351 ± .010	<b>.353</b> ± .011
		Unsupervised	.185 ± .031	<b>.246</b> ± .017	.235 ± .016	.272 ± .015	<b>.276</b> ± .007	.259 ± .027
		Supervised	.230 ± .073	.332 ± .030	<b>.425</b> ± .018	.708 ± .036	.609 ± .022	<b>.722</b> ± .023
	Pose	No	<b>.570</b> ± .066	—	—	<b>.795</b> ± .046	—	—
		Unsupervised	.436 ± .057	.594 ± .032	<b>.659</b> ± .036	.737 ± .077	.638 ± .024	<b>.778</b> ± .062
	Supervised	Supervised	.725 ± .083	.832 ± .010	<b>.882</b> ± .017	.914 ± .030	.871 ± .019	<b>.952</b> ± .014
		Video	No	.541 ± .038	.577 ± .017	<b>.693</b> ± .017	.651 ± .023	.658 ± .011
	Multimodal	No	<b>.670</b> ± .048	—	—	<b>.825</b> ± .023	—	—
Unsupervised		.574 ± .045	.740 ± .016	<b>.774</b> ± .018	.786 ± .026	.788 ± .023	<b>.866</b> ± .019	
Supervised		.744 ± .053	.917 ± .007	<b>.932</b> ± .011	.945 ± .023	.941 ± .008	<b>.965</b> ± .012	

Table 2: Comparison of classification results for the MM-Fit test dataset (mean Macro  $F_1$ -Scores and standard deviations). Results demonstrating superior performance are highlighted in bold. A “—” indicates that we were not able to produce meaningful results.

We evaluate our method on all 7,200 real-world videos from Flag3D. To prepare the data, we follow the same approach as described in Section 3.2: First, we convert the videos to 50 fps. Then, we extract CLIP video features, ADA text embeddings, virtual sensor data, and poses (VideoPose3D) with IMUTube. We discard 943 videos for which IMUTube was unable to generate any sensor data. For the remaining 6,257 videos, we retrieve cumulatively over 21 hours of useful data. We split the data based on the person IDs performing the exercises into train (5 persons), validation (2 persons), and test (3 persons) sets. We apply a sliding window with a window size of 100 frames (2 seconds) and a step size of 50 frames (1 second). We also evaluate our method on a subset of 7,200 rendered videos, from which IMUTube was capable to extract sensor data for 6,832 videos (totaling 24 hours), processing them analogously to the real-world videos.

### 5.1.2 MM-Fit

The MM-Fit Strömbäck et al. [2020] dataset includes multi-view RGB-D video recordings, accompanied by 3D pose estimations extracted from single-view RGB frames with OpenPose and VideoPose3D. Additionally, it comprises a comprehensive compilation of time-synchronized inertial sensor data sourced from two smartphones, two smartwatches, and a earbud worn by participants during workout sessions. 10 Participants performed 21 full-body workout routines in total while positioned in front of two depth cameras, with five smart devices strategically placed to collect inertial sensor data. The task is delimited to the recognition of exercises performed by individual participants. Thus, each workout session involves a solitary participant. This setup is tailored for home workout environments. Each workout session encompasses three sets of 10 exercises, with 10 repetitions for each exercise. The selected exercises encompass well-known resistance training routines, including squats, lunges (with dumbbells), alternating-arm bicep curls, sit-ups, push-ups, seated overhead dumbbell triceps extensions, standing dumbbell rows, jumping jacks, seated dumbbell shoulder press, and dumbbell lateral shoulder raises.

We conduct the same preprocessing steps as for our dataset and FLAG3D but solely extract ADA text embeddings and CLIP video features. For pose and sensor, we utilize the 3D pose and Smartwatch accelerometer data of the left and right wrist provided by MM-Fit. Furthermore, we consider two scenarios: training the classifiers with and without including the “No Activity” category. Additionally, we calibrate sensor and pose data using a probability integral transform function Conover and Iman [1981], following the implementation of Kwon et al. [2021]. In the unsupervised setting, all real data is calibrated with the virtual train data; whereas in the supervised case, label information is utilized to perform the calibration separately for each class.



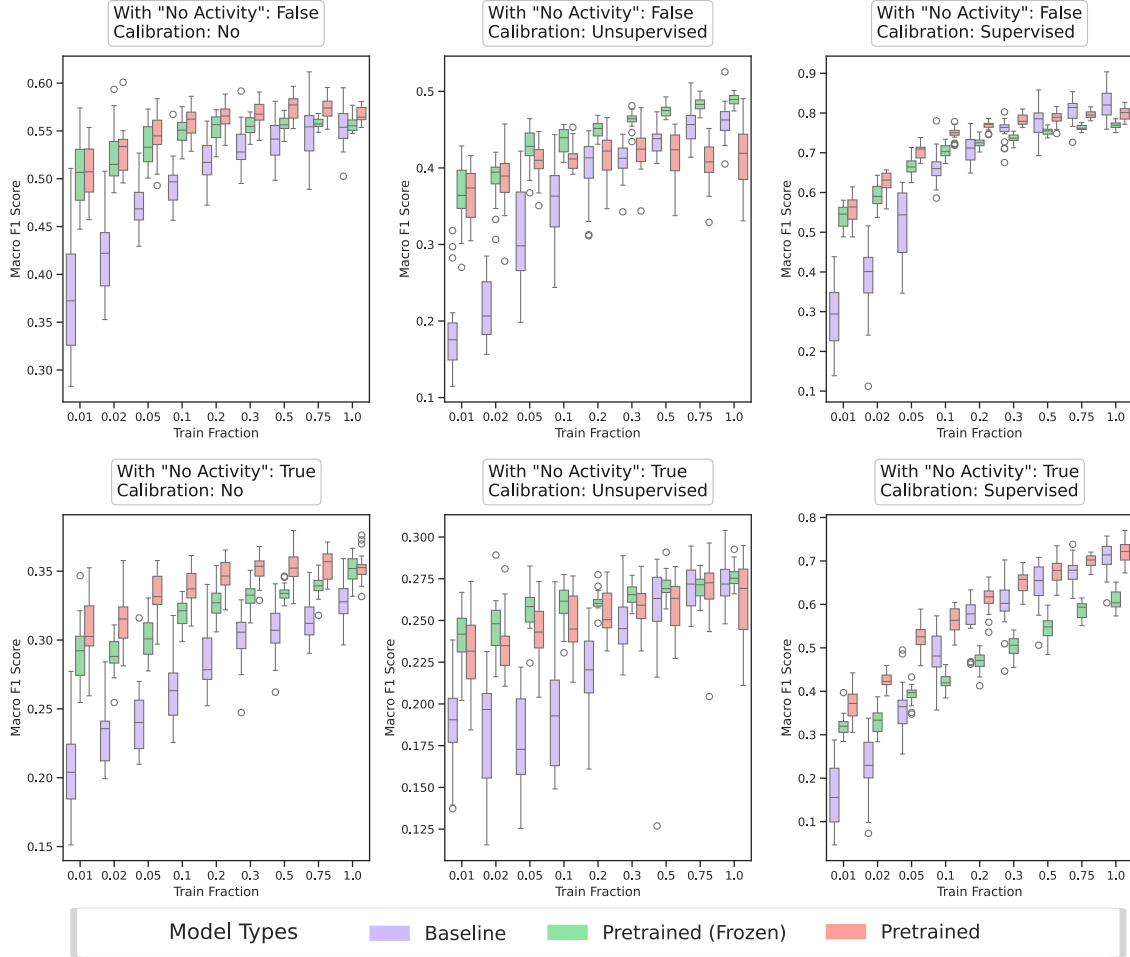


Figure 4: Boxplots visualizing the classification performance (Macro  $F_1$ -Score) across various training data fractions of the baseline model versus models with a pretrained encoder and projection, both frozen and unfrozen, on MM-Fit Smartwatch (left and right wrist) accelerometer data.

## 5.2 Evaluation of Generalization Performance on Unseen Datasets

To evaluate performance in a more realistic scenario, we measure the model’s capability to match input modalities with the correct labels of the MM-Fit dataset in the scenario where the dataset is unseen. For that, we first calculate the ADA text embeddings  $v_{text}^l$  for all labels  $l$  of the MM-Fit dataset. For the “No Activity” class, which doesn’t correspond to a specific activity, we generate its embedding by taking the mean of the embeddings of all labels. For a given data sample  $v_m$  of input modality  $m$ , we then choose labels based on the closest similarity score  $sim(v_{text}^l, v_m)$  by calculating  $\text{argmin}_l sim(v_{text}^l, v_m)$  for all labels  $l$ .

## 6 Results

### 6.1 FLAG3D

Table 1 demonstrates that the pretrained model consistently outperforms the baseline across all input modalities with respect to Macro  $F_1$ -Score on both the real-world and the rendered dataset when utilizing either 2% or 100% of the training data. When comparing the baseline to our unfrozen pretrained model across both datasets and all types of input, we observe an absolute performance increase ranging from 0.042 (rendered dataset, video input) to 0.219 (real-world, multimodal) with just 2% of the training data. For the full dataset (100% of the training data), the improvement spans from 0.029 (real-world, video) to 0.208 (real-world, multimodal). This indicates that our pretrained encoders have learned a robust representation of the respective input modality, thereby enhancing classification performance even on a

new dataset. We expect that our pretrained, unfrozen encoders would outperform the frozen ones by adapting more effectively to the training data. This expectation was confirmed in 7 out of 8 scenarios when using the full dataset for training, with a absolute performance increase of 0.014 on average. However, with only 2% of the training data, the frozen encoders show even superior performance in 3 out of 8 scenarios, and the unfrozen encoders do not perform significantly better on average, suggesting that the pretrained representation could not be enhanced with such a limited amount of training data. Generally, poses perform best out of all input modalities. While the multimodal setting does not show substantial improvement for the rendered dataset, a slight enhancement (0.015 for 2% train and 0.028 for 100% train) is observed for our pretrained, unfrozen model in the real-world setting when concatenating all modalities, compared to just using poses as input.

From the boxplots presented in Figure 3, which compare the performance of the models across all modalities and various training fractions ranging from 1% to 100%, we observe that the pretrained models significantly outperform the baseline for all training fractions and most modalities. The only exception is the video modality, which performed worse out of all modalities and only slightly better than the baseline. However, with a limited amount of training data, our model demonstrates better performance relative to the baseline in the classification task over all modalities.

## 6.2 MM-Fit

Table 2 presents the results of experiments conducted with and without the inclusion of the “No Activity” class, across all input modalities and calibration configurations (none, unsupervised, and supervised), for both 2% and 100% training data fractions. We find that applying supervised, per class calibration generally enhances performance, whereas unsupervised calibration tends to diminish performance for sensor input. For pose data and multimodal inputs (which include poses), our pretrained encoders are unable to yield results without calibration—the training loss failed to decrease, remaining at infinity for 25 epochs. Notably, both IMUTube and MM-Fit utilize VidePose3D for pose extraction, but IMUTube incorporates extensive additional pre- and post-processing steps. Given that our pretraining utilized these poses generated by IMUTube, we speculate that our pose representation learned is significantly different from that of the MM-Fit poses. This difference likely hinders the model’s ability to learn when no calibration is performed. Indeed, calibration rectifies this issue. Excluding the scenarios without calibration for pose and multimodal inputs, our method surpasses the baseline in almost every case. The only exception is observed when training with sensor input and 100% training data, excluding the “No Activity” class and applying supervised calibration, where the baseline achieves a slightly better result (0.822 versus 0.798), which is due to the fact that MM-Fit uses real, rather than simulated sensor data.

Leveraging multimodal inputs (i.e., concatenating all modalities) achieves the highest performance, suggesting that HAR benefits from the diverse perspectives of multiple modalities. In this multimodal scenario, our method, compared to the baseline, improves the Macro  $F_1$ -Score from 0.945 to 0.965 (with “No Activity”) and from 0.973 to 0.999 (without “No Activity”) when trained on the full dataset. Furthermore, with only 2% of the training data available, we improve performance from 0.744 to 0.932 (with “No Activity”) and from 0.819 to 0.992 (without “No Activity”). These findings show that our model has significantly better performance compared to the baseline and learns more efficiently when only a small amount of training data is available.

Figure 4 illustrates boxplots that exemplify the classification performances on accelerometer data input for all training fractions. It shows that our model significantly outperforms the baseline when trained with a minimal amount of training data, and generally, we observe a notable reduction in variance for our pretrained models compared to the baseline. This suggests that our pretrained sensor encoder has effectively learned a meaningful representation of real accelerometer data.

Table 3 demonstrates the generalization performance of our representation on MM-Fit in the scenario where the dataset is unseen. In this analysis, we contrast the outcomes of unimodal training—where models were individually trained to align sensor-text, pose-text, and video-text—with those of multimodal training, where we tasked a single model to align all four modalities concurrently. Our findings reveal that, after implementing supervised calibration for pose and sensor modalities, our model surpasses random chance performance in all but one scenario. The peak top-1 performance achieves a Macro  $F_1$ -Score of 0.638 for pose input. The only exception is the accelerometer input when the “No Activity” category is included. In this case, the top-1 performance is 0.085 for unimodal and 0.080 for multimodal training, both of which are less than  $\frac{11}{100} = 0.11$ . This is also the only instance where multimodal training does not yield a performance enhancement, being outperformed by a small margin of 0.005. Conversely, in all other training configurations, multimodal training demonstrates superior performance over unimodal training. On average, multimodal training increases the performance by 0.069 (top-1). This supports our narrative that multimodal training can augment the model’s comprehension of various inputs.

	Input Modality	Calibration	Macro $F_1$ -Score					
			Unimodal Training			Multimodal Training		
			Top-1	Top-3	Top-5	Top-1	Top-3	Top-5
With "No Act."	Pose	No	.006	.188	.370	.006	.188	.370
		Unsupervised	.098	.159	.330	.051	.192	.420
		Supervised	.280	.366	.471	.306	.615	.920
	Video	No	.165	.405	.576	.291	.481	.661
		Unsupervised	.035	.145	.346	.017	.151	.413
		Supervised	.058	.309	.488	.022	.124	.333
Without "No Act."	Pose	No	.027	.233	.443	.027	.233	.444
		Unsupervised	.151	.335	.498	.083	.225	.515
		Supervised	.618	.816	.903	.638	.869	.959
	Video	No	.291	.603	.677	.535	.631	.684
		Unsupervised	.099	.250	.445	.033	.229	.547
		Supervised	.059	.336	.510	.048	.176	.339
Sensor	No	.133	.386	.624	.137	.378	.631	
	Unsupervised							
	Supervised							

Table 3: Results (Macro  $F_1$ -Scores) for the generalization performance of our representation on MM-Fit dataset in the scenario where the dataset is unseen.

## 7 Conclusion

In this study, we have developed a novel approach to HAR by introducing a joint feature space that integrates video, pose, simulated accelerometer, and textual data. Our model was trained on a large, self-created multimodal fitness dataset containing over 78 hours of recordings. We evaluated our method using the FLAG3D dataset and the MM-Fit dataset. On MM-Fit, our model achieved an impressive Macro  $F_1$ -Score of up to 0.992 with only 2% of the train data and 0.999 when all available training data was used. Moreover, in the scenario where the MM-Fit dataset was unseen, we demonstrated a generalization performance of up to 0.638. Our results reveal that our pretrained encoders effectively capture a meaningful representation for recognizing human activities. Furthermore, our approach not only demonstrates impressive results on an unseen dataset but also is capable of enhancing performance when applied to real-world sensor data.

## References

- Jay-Shian Tan, Behrouz Khabbaz Beheshti, Tara Binnie, Paul Davey, JP Caneiro, Peter Kent, Anne Smith, Peter O’Sullivan, and Amity Campbell. Human activity recognition for people with knee osteoarthritis—a proof-of-concept. *Sensors*, 21(10):3381, 2021.
- Kristina Host and Marina Ivašić-Kos. An overview of human action recognition in sports based on computer vision. *Heliyon*, page e09633, 2022.
- Amir Nadeem, Ahmad Jalal, and Kibum Kim. Accurate physical activity recognition using multidimensional features and markov model for smart health fitness. *Symmetry*, 12(11):1766, 2020.
- Ajeet Sunil, Manav Hiren Sheth, E Shreyas, et al. Usual and unusual human activity recognition in video using deep learning and artificial intelligence for security applications. In *2021 Fourth International Conference on Electrical, Computer and Communication Technologies (ICECCT)*, pages 1–6. IEEE, 2021.
- Lasitha Piyathilaka and Sarath Kodagoda. Human activity recognition for domestic robots. In *Field and Service Robotics: Results of the 9th International Conference*, pages 395–408. Springer, 2015.
- Rebeen Ali Hamad, Wai Lok Woo, Bo Wei, and Longzhi Yang. Overview of human activity recognition using sensor data. *arXiv preprint arXiv:2309.07170*, 2023.
- Alec Radford, Jong Wook Kim, Chris Hallacy, Aditya Ramesh, Gabriel Goh, Sandhini Agarwal, Girish Sastry, Amanda Askell, Pamela Mishkin, Jack Clark, et al. Learning transferable visual models from natural language supervision. In *International conference on machine learning*, pages 8748–8763. PMLR, 2021.
- Josh Achiam, Steven Adler, Sandhini Agarwal, Lama Ahmad, Ilge Akkaya, Florencia Leoni Aleman, Diogo Almeida, Janko Altmenschmidt, Sam Altman, Shyamal Anadkat, et al. Gpt-4 technical report. *arXiv preprint arXiv:2303.08774*, 2023.
- Shing Chan, Hang Yuan, Catherine Tong, Aidan Acquah, Abram Schonfeldt, Jonathan Gershuny, and Aiden Doherty. Capture-24: A large dataset of wrist-worn activity tracker data collected in the wild for human activity recognition, 2024.

- Hyeokhyen Kwon, Bingyao Wang, Gregory D. Abowd, and Thomas Plötz. Approaching the real-world: Supporting activity recognition training with virtual imu data. *Proc. ACM Interact. Mob. Wearable Ubiquitous Technol.*, 5(3), sep 2021.
- Zhe Cao, Tomas Simon, Shih-En Wei, and Yaser Sheikh. Realtime multi-person 2d pose estimation using part affinity fields. In *Proceedings of the IEEE conference on computer vision and pattern recognition*, pages 7291–7299, 2017.
- Dario Pavllo, Christoph Feichtenhofer, David Grangier, and Michael Auli. 3d human pose estimation in video with temporal convolutions and semi-supervised training. In *Proceedings of the IEEE/CVF conference on computer vision and pattern recognition*, pages 7753–7762, 2019.
- David Strömbäck, Sangxia Huang, and Valentin Radu. Mm-fit: Multimodal deep learning for automatic exercise logging across sensing devices. *Proc. ACM Interact. Mob. Wearable Ubiquitous Technol.*, 4(4), dec 2020.
- Jennifer R Kwapisz, Gary M Weiss, and Samuel A Moore. Activity recognition using cell phone accelerometers. *ACM SigKDD Explorations Newsletter*, 12(2):74–82, 2011.
- Francisco Javier Ordóñez and Daniel Roggen. Deep convolutional and lstm recurrent neural networks for multimodal wearable activity recognition. *Sensors*, 16(1):115, 2016.
- Sakorn Mekruksavanich and Anuchit Jitpattanakul. Multimodal wearable sensing for sport-related activity recognition using deep learning networks. *Journal of Advances in Information Technology*, 2022.
- Momal Ijaz, Renato Diaz, and Chen Chen. Multimodal transformer for nursing activity recognition. In *Proceedings of the IEEE/CVF Conference on Computer Vision and Pattern Recognition*, pages 2065–2074, 2022.
- Michael Duhme, Raphael Memmesheimer, and Dietrich Paulus. Fusion-gcn: Multimodal action recognition using graph convolutional networks. In *Pattern Recognition: 43rd DAGM German Conference, DAGM GCPR 2021, Bonn, Germany, September 28–October 1, 2021, Proceedings*, pages 265–281. Springer, 2022.
- Mirco Plananamente, Chiara Plizzari, and Barbara Caputo. Test-time adaptation for egocentric action recognition. In *Image Analysis and Processing–ICIAP 2022: 21st International Conference, Lecce, Italy, May 23–27, 2022, Proceedings, Part III*, pages 206–218. Springer, 2022.
- Md Milon Islam, Sheikh Nooruddin, Fakhri Karray, and Ghulam Muhammad. Human activity recognition using tools of convolutional neural networks: A state of the art review, data sets, challenges, and future prospects. *Computers in Biology and Medicine*, page 106060, 2022.
- Paul Hongsuck Seo, Arsha Nagrani, and Cordelia Schmid. Look before you speak: Visually contextualized utterances. In *Proceedings of the IEEE/CVF Conference on Computer Vision and Pattern Recognition*, pages 16877–16887, 2021.
- Chen Sun, Austin Myers, Carl Vondrick, Kevin Murphy, and Cordelia Schmid. Videobert: A joint model for video and language representation learning. In *Proceedings of the IEEE/CVF international conference on computer vision*, pages 7464–7473, 2019.
- Linjie Li, Yen-Chun Chen, Yu Cheng, Zhe Gan, Licheng Yu, and Jingjing Liu. Hero: Hierarchical encoder for video+language omni-representation pre-training. *arXiv preprint arXiv:2005.00200*, 2020.
- Antoine Miech, Jean-Baptiste Alayrac, Lucas Smaira, Ivan Laptev, Josef Sivic, and Andrew Zisserman. End-to-end learning of visual representations from uncurated instructional videos. In *Proceedings of the IEEE/CVF Conference on Computer Vision and Pattern Recognition*, pages 9879–9889, 2020.
- Jian-Fang Hu, Wei-Shi Zheng, Lianyang Ma, Gang Wang, Jianhuang Lai, and Jianguo Zhang. Early action prediction by soft regression. *IEEE transactions on pattern analysis and machine intelligence*, 41(11):2568–2583, 2018.
- Amir Zadeh, Minghai Chen, Soujanya Poria, Erik Cambria, and Louis-Philippe Morency. Tensor fusion network for multimodal sentiment analysis. *arXiv preprint arXiv:1707.07250*, 2017.
- Jiasen Lu, Dhruv Batra, Devi Parikh, and Stefan Lee. Vilbert: Pretraining task-agnostic visiolinguistic representations for vision-and-language tasks. *Advances in neural information processing systems*, 32, 2019.
- Hu Xu, Gargi Ghosh, Po-Yao Huang, Dmytro Okhonko, Armen Aghajanyan, Florian Metze, Luke Zettlemoyer, and Christoph Feichtenhofer. Videoclip: Contrastive pre-training for zero-shot video-text understanding. *arXiv preprint arXiv:2109.14084*, 2021.
- Hongwei Xue, Yuchong Sun, Bei Liu, Jianlong Fu, Ruihua Song, Houqiang Li, and Jiebo Luo. Clip-vip: Adapting pre-trained image-text model to video-language representation alignment. *arXiv preprint arXiv:2209.06430*, 2022.
- Uriel Singer, Adam Polyak, Thomas Hayes, Xi Yin, Jie An, Songyang Zhang, Qiyan Hu, Harry Yang, Oron Ashual, Oran Gafni, et al. Make-a-video: Text-to-video generation without text-video data. *arXiv preprint arXiv:2209.14792*, 2022.

- Guy Tevet, Brian Gordon, Amir Hertz, Amit H Bermano, and Daniel Cohen-Or. Motionclip: Exposing human motion generation to clip space. In *Computer Vision—ECCV 2022: 17th European Conference, Tel Aviv, Israel, October 23–27, 2022, Proceedings, Part XXII*, pages 358–374. Springer, 2022.
- Seungwhan Moon, Andrea Madotto, Zhaojiang Lin, Alireza Dirafzoon, Aparajita Saraf, Amy Bearman, and Babak Damavandi. Imu2clip: Multimodal contrastive learning for imu motion sensors from egocentric videos and text. *arXiv preprint arXiv:2210.14395*, 2022.
- Jake K Aggarwal and Michael S Ryoo. Human activity analysis: A review. *Acm Computing Surveys (Csur)*, 43(3): 1–43, 2011.
- Mengmeng Wang, Jiazheng Xing, and Yong Liu. Actionclip: A new paradigm for video action recognition. *arXiv preprint arXiv:2109.08472*, 2021.
- Zehua Sun, Qihong Ke, Hossein Rahmani, Mohammed Bennamoun, Gang Wang, and Jun Liu. Human action recognition from various data modalities: A review. *IEEE transactions on pattern analysis and machine intelligence*, 45(3):3200–3225, 2022.
- Md Golam Morshed, Tangina Sultana, Aftab Alam, and Young-Koo Lee. Human action recognition: A taxonomy-based survey, updates, and opportunities. *Sensors*, 23(4):2182, 2023.
- Rohit Girdhar, Alaaeldin El-Nouby, Zhuang Liu, Mannat Singh, Kalyan Vasudev Alwala, Armand Joulin, and Ishan Misra. Imagebind: One embedding space to bind them all. In *Proceedings of the IEEE/CVF Conference on Computer Vision and Pattern Recognition*, pages 15180–15190, 2023.
- Saining Xie, Chen Sun, Jonathan Huang, Zhuowen Tu, and Kevin Murphy. Rethinking spatiotemporal feature learning: Speed-accuracy trade-offs in video classification. In *Proceedings of the European conference on computer vision (ECCV)*, pages 305–321, 2018.
- Jacob Devlin, Ming-Wei Chang, Kenton Lee, and Kristina Toutanova. Bert: Pre-training of deep bidirectional transformers for language understanding. *arXiv preprint arXiv:1810.04805*, 2018.
- Chuan Guo, Shihao Zou, Xinxin Zuo, Sen Wang, Wei Ji, Xingyu Li, and Li Cheng. Generating diverse and natural 3d human motions from text. In *Proceedings of the IEEE/CVF Conference on Computer Vision and Pattern Recognition*, pages 5152–5161, 2022.
- Yansong Tang, Jinpeng Liu, Aoyang Liu, Bin Yang, Wenxun Dai, Yongming Rao, Jiwen Lu, Jie Zhou, and Xiu Li. Flag3d: A 3d fitness activity dataset with language instruction. In *Proceedings of the IEEE/CVF Conference on Computer Vision and Pattern Recognition*, pages 22106–22117, 2023.
- W. J. Conover and Ronald L. Iman. Rank transformations as a bridge between parametric and nonparametric statistics. *The American Statistician*, 35(3):124–129, 1981. ISSN 00031305.